applied sciences

MDPI

Article

Pituitary Structural and Vascular Changes with Preserved Hypothalamic Microstructure in Postmenopausal Women with Primary Sjögren's Syndrome: An MRI Study

Anastasia Zikou [1], Artemis Andrianopoulou [1], Effrosyni Styliara [1], Nikolaos Koletsos [2], Nafsika Gerolimatou [2], Loukas Astrakas [3], George Alexiou [4,*], Paraskevi Voulgari [2], Dimitrios N. Kiortsis [1] and Maria Argyropoulou [1]

[1] Department of Clinical Radiology and Imaging, Faculty of Medicine, School of Health Sciences, University of Ioannina, 45500 Ioannina, Greece; anzikou@uoi.gr (A.Z.); artemisandrianopoulou@gmail.com (A.A.); effrosynistyliara@gmail.com (E.S.); dkiorts@uoi.gr (D.N.K.); margyrop@uoi.gr (M.A.)
[2] Department of Rheumatolog, Faculty of Medicine, School of Health Sciences, University of Ioannina, 45500 Ioannina, Greece; nick.koletsos@gmail.com (N.K.); gnafsika@gmail.com (N.G.); pvoulgar@uoi.gr (P.V.)
[3] Department of Medical Physics, Faculty of Medicine, School of Health Sciences, University of Ioannina, 45500 Ioannina, Greece; astrakas@uoi.gr
[4] Department of Neurosurgery, Faculty of Medicine, School of Health Sciences, University of Ioannina, 45500 Ioannina, Greece
* Correspondence: galexiou@uoi.gr

Abstract

(1) Background: This study aimed to evaluate hypothalamic–hypophyseal (HH) axis involvement in Primary Sjögren's syndrome (pSS) using MRI and assess its relationship with hypothalamic–pituitary–adrenal (HPA) axis dysfunction. (2) Methods: A total of 22 postmenopausal women with pSS and 17 healthy controls were enrolled. Midline sagittal T1-weighted MRI was used to measure pituitary gland height (PGH). Dynamic contrast-enhanced imaging assessed hypothalamic–hypophyseal (HH) microcirculation, while diffusion tensor imaging (DTI) evaluated hypothalamic microstructure. Biochemical variables, including cortisol and complement factors, were measured. Linear regression analysis was performed to identify predictors of PGH. (3) Results: Patients had a mean disease duration of 11.5 ± 6.7 years. PGH was significantly different in patients than in controls (3.6 ± 1.1 mm vs. 4.4 ± 0.6 mm, $p = 0.004$). Cortisol levels were also reduced (8.9 ± 4.6 µg/dL vs. 12.6 ± 4.7 µg/dL, $p = 0.040$), while ACTH levels were not significantly different. Dynamic imaging demonstrated delayed enhancement of the anterior pituitary lobe. DTI revealed no hypothalamic microstructural abnormalities. PGH was positively associated with C3 ($p = 0.029$). (4) Conclusions: pSS is associated with pituitary structural and functional alterations consistent with HPA axis hypofunction, likely reflecting immune-mediated pituitary involvement with preserved hypothalamic integrity.

Keywords: MRI; Primary Sjögren's syndrome; hypothalamic–hypophyseal axis; hypothalamic–pituitary–adrenal axis; pituitary gland height

Check for updates

Academic Editor: Vladislav Toronov

Received: 1 May 2026
Revised: 12 June 2026
Accepted: 17 June 2026
Published: 23 June 2026

Copyright: © 2026 by the authors. Licensee MDPI, Basel, Switzerland. This article is an open access article distributed under the terms and conditions of the Creative Commons Attribution (CC BY) license.

1. Introduction

Primary Sjögren's syndrome (pSS) is a chronic autoimmune disorder characterized predominantly by lymphocytic infiltration of the exocrine glands, leading to symptoms such as xerostomia and keratoconjunctivitis sicca. However, the disease extends beyond glandular involvement, with systemic manifestations affecting multiple organ systems, including the central nervous system [1–4].

Magnetic resonance imaging (MRI) studies investigating central nervous system involvement in pSS have demonstrated focal white matter hyperintensities, as well as reductions in both gray matter and white matter (WM) volumes across various brain regions. In addition, diffusion tensor imaging has revealed widespread microstructural WM abnormalities [5–7]. These findings are thought to reflect underlying inflammatory and ischemic vasculopathy observed in histopathological studies [8]. Furthermore, functional MRI studies have identified altered functional connectivity, particularly within the somatosensory cortex, along with WM microstructural changes associated with depressive symptoms in patients with pSS [9]. Resting-state functional MRI has also demonstrated abnormal brain activity in regions such as the visual cortex and the frontoparietal junction [10]. Evidence suggests that pSS may also involve neuroendocrine dysregulation, particularly affecting the hypothalamic–pituitary–adrenal (HPA) axis, a key regulator of stress responses and immune function [11]. Previous studies have reported HPA axis hypofunction in pSS, characterized by altered cortisol secretion patterns and impaired stress responses, which may contribute to disease pathogenesis and symptom severity [12,13]. Despite these observations, the neuroanatomical correlates underlying HPA axis dysfunction in pSS remain poorly defined. MRI, with its ability to assess both structural and microstructural properties of the hypothalamic–hypophyseal (HH) axis, offers a promising approach for investigating potential morphological alterations associated with HPA axis dysfunction [14]. However, to date, no MRI studies have specifically evaluated the HH axis in pSS in terms of morphology and microstructure and their relationship with clinical and hormonal markers of HPA axis function. Elucidating these associations may enhance our understanding of neuroendocrine involvement in pSS.

The present study aimed to assess the morphological and microstructural characteristics of the HH axis in patients with pSS using MRI, with a particular focus on identifying alterations associated with HPA axis hypofunction. We hypothesized that microvascular or autoimmune neuroinflammatory processes may be associated with subtle structural or microstructural changes in the HH axis, potentially contributing to endocrine dysregulation.

2. Materials and Methods

2.1. Subjects

This cross-sectional study included 22 female patients with pSS and 17 age- and sex-matched healthy controls. All participants were postmenopausal to eliminate the confounding effects of the menstrual cycle. Demographic and epidemiological data (including age, sex, and disease duration) were recorded for all participants, and a comprehensive clinical examination was performed. Non-exocrine manifestations, as well as a medical history of hypothyroidism and other comorbidities, were documented. All participants underwent standardized morning laboratory testing, including hormonal evaluation (prolactin, estradiol, luteinizing hormone [LH], testosterone, adrenocorticotropic hormone [ACTH], dehydroepiandrosterone sulfate [DHEA-S], progesterone, cortisol, and insulin-like growth factor 1 [IGF-1]). Morning basal ACTH and cortisol concentrations were obtained as measures of HPA axis activity. Dynamic endocrine testing was not included in the study protocol. Immunological testing, including antinuclear antibodies and rheumatoid factor, was also performed.

The diagnosis of pSS was established according to the American College of Rheumatology (ACR) and the European Alliance of Associations for Rheumatology (EULAR) classification criteria for pSS [15]. The presence of other connective tissue diseases was excluded, and only patients with pSS were included in the study. Exclusion criteria included a history or clinical evidence of cardiovascular disease, peripheral arterial disease, hepatic dysfunction (transaminase levels > 1.5 times the upper limit of normal), renal insuf-

ficiency (serum creatinine > 1.6 mg/dL), proteinuria (>0.5 g/day), diabetes mellitus (fasting plasma glucose $\geq$ 126 mg/dL or use of antidiabetic medication), hypertension (blood pressure > 140/90 mmHg or use of antihypertensive medication), thyroid-stimulating hormone > 5 mU/mL, dyslipidemia, corticosteroid use within the previous 6 months, and a history of neurological disorders (including autoimmune or demyelinating diseases, migraine, head injury, or Alzheimer's disease). All participants underwent the Mini-Mental State Examination; none scored $\leq$ 23, which would indicate cognitive impairment and warrant exclusion. The exclusion criteria were implemented to minimize vascular and neurological-related confounding factors and to better isolate the effects of the disease under investigation on pituitary structure. The study was approved by the institutional review board (No. 2669/24-02-2016) and the university hospital ethics committee (No. 328/12-5-2026). Written informed consent was obtained from all participants.

2.2. Imaging Protocol and Measurements

All MR imaging examinations were performed on the same 1.5T unit (Gyroscan Intera; Philips Healthcare, Best, The Netherlands) using a quadrature head coil.

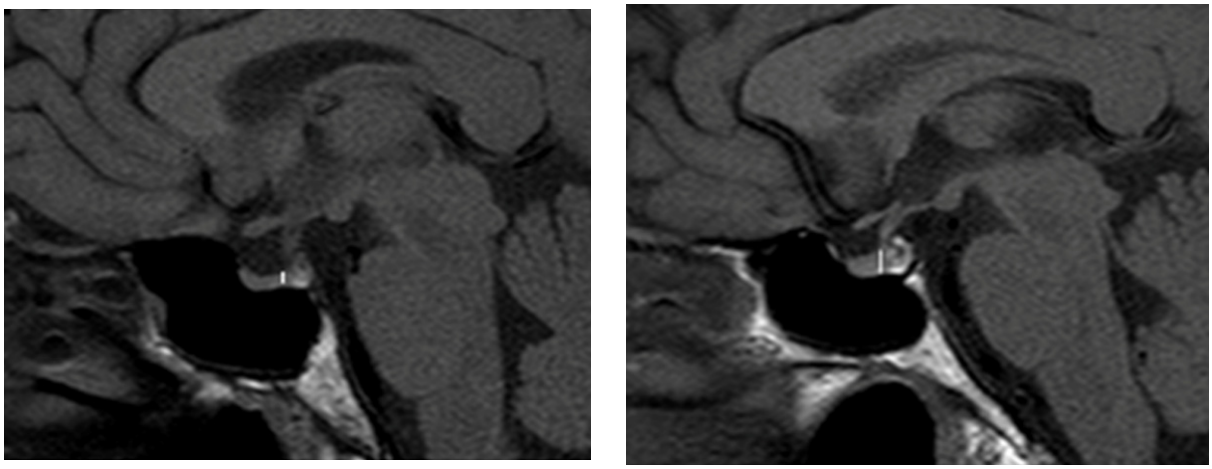
The imaging protocol of the HH axis included the following:

(1) T1-weighted spin-echo images on the sagittal plane (TR: 650 ms, TE: 17 ms, matrix: 256 $\times$ 256, two excitations, slice thickness: 3 mm, gap: 0.3 mm, FOV: 23 cm) were used for structural pituitary imaging. Pituitary gland height (PGH) was evaluated on a T1-weighted midline sagittal scan. PGH was selected as the primary morphological metric because it is highly reproducible and serves as a reliable clinical surrogate for overall gland size [16]. This measurement approach minimizes the volumetric calculation errors and partial volume effects that can occur when attempting manual 3D segmentation of the pituitary's lateral borders, particularly at a 1.5T field strength [17]. The PGH was measured perpendicular to the floor of the sella turcica on a midline sagittal T1-weighted image (Figure 1).

(2) A dynamic contrast-enhanced sequence was performed on the sagittal plane following bolus injection of Gd-DTPA at 0.1 mmol/kg body weight, administered via a 20-gauge needle at the start of the first acquisition. A fast-framing technique was used, with 20 sagittal scans sequentially acquired, each lasting 7.2 s, with technical parameters set to TR: 4.5 ms, TE: 1.35 ms, matrix: 124 $\times$ 124, and FOV: 25 cm, totaling 2 min and 24 s to assess the vascularization of the HH axis. Enhancement curves were generated by placing small (1–2 mm^2) ROIs on the posterior and anterior pituitary lobes, the tuber cinereum, and the straight sinus as a reference [18,19] (Figure 2).

(3) DTI: A single-shot multisection spin-echo echo-planar sequence (TR: 9807 ms, TE: 131 ms, FOV: 230 mm, matrix: 128 $\times$ 128, section thickness: 2.5 mm, maximum b-value: 800 s/mm^2, 16 noncollinear diffusion directions, scanning time: 5 min and 34 s, inter-slice gap: 0) was utilized to assess the microstructure of the HH axis. Due to the lack of atlases that precisely delineate hypothalamic nuclei, a manual ROI-based analysis was selected to ensure reliable anatomical localization within the hypothalamic structure, using the methodology described by Baroncini et al. [20]. In this approach, the hypothalamus is divided into anatomical regions (e.g., anterior, posterior), with the coordinates of their central voxels provided [21]. ADC (apparent diffusion coefficient) values were obtained in 5 regions of interest (ROIs): anterior and posterior parts of the right and left hypothalami and the lateral ventricle for the ADC of the cerebrospinal fluid (CSF). The surface of the ROIs was 3 mm^2, for a slice thickness of 2.5 mm. A single rater placed the diffusion ROIs. The anatomical delineation of the hypothalamic region on ADC maps was established by the rater in consensus with a senior neuroradiologist following dedicated training. The ADC values were

obtained bilaterally in the anterior and posterior parts of the hypothalamus, averaged, and normalized to the ADC values from the CSF (ADC hypothalamus/ADC CSF).



(**a**) (**b**)

Figure 1. PGH was measured perpendicular to the sella turcica floor on a midline sagittal T1 image: 2.6 mm in a 63-year-old patient (**a**); 3.8 mm in a 68-year-old control (**b**).

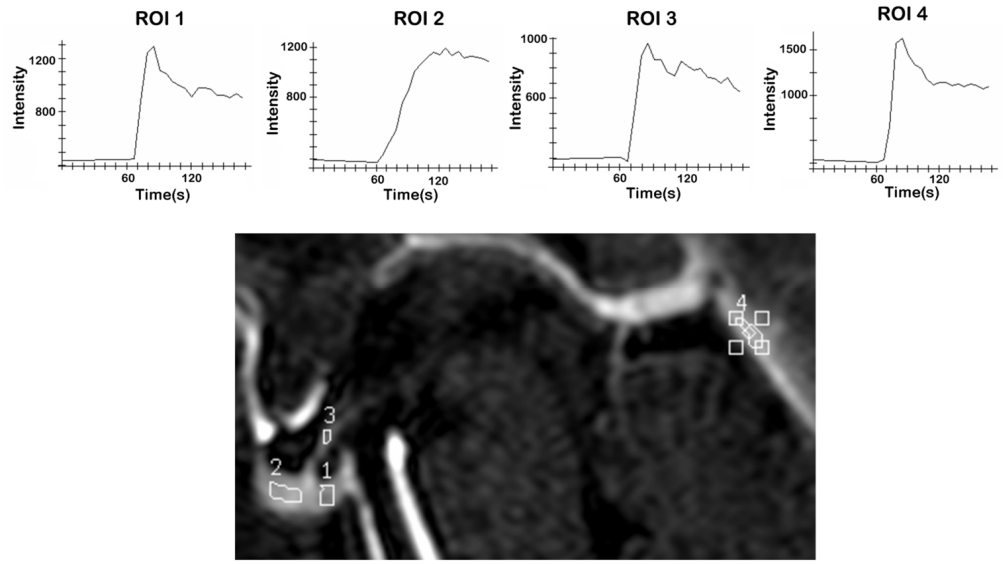


Figure 2. Dynamic contrast-enhanced sagittal imaging: enhancement curves were obtained using ROIs placed on the posterior (ROI 1) and anterior (ROI 2) pituitary lobes, the tuber cinereum (ROI 3), and the straight sinus as reference (ROI 4). The ROI 2 curve shows delayed enhancement in the anterior pituitary lobe.

2.3. Statistical Analysis

Continuous variables were tested for normality using the Shapiro–Wilk test. As all variables were normally distributed ($p > 0.05$), between-group comparisons across demographic, imaging, and clinical parameters were performed using independent-samples *t*-tests, with Levene's test applied to assess homogeneity of variances. Data are presented as mean ± standard deviation.

Linear regression analysis was conducted in the patient group to identify independent predictors of PGH. The initial model was heavily parameterized to ensure clinical and systemic specificity, entering the following candidate variables: age, disease duration, cortisol, ACTH, DHEA-S, prolactin, LH, C3, and C4. To optimize model fit and avoid over-

parameterization within our sample size, variables with a p-value ≥ 0.10 were sequentially removed during a stepwise elimination process if they failed to provide unique explanatory power for the variance in PGH.

Statistical significance was set at $p < 0.05$. All analyses were performed using IBM SPSS Statistics (version 26.0; IBM Corp., Armonk, NY, USA). Given the pilot nature and small sample size of this study, the univariate comparisons are fundamentally exploratory and intended for hypothesis generation. Consequently, results are reported without formal multiple-comparison corrections to maintain transparency and highlight trend-level variations.

3. Results

There was no significant difference in age between patients and controls (67.2 ± 7.1 vs. 63.6 ± 5.1 years, $p = 0.092$). The mean disease duration in patients was 11.5 ± 6.7 years (Table 1).

Table 1. Descriptive statistics of demographics, imaging, and clinical data, and *t*-test comparison results between patient and healthy control groups.

Variable [1]	Patients (Mean ± SD)	Controls (Mean ± SD)	*p* Value (*t*-Test)
Age (years)	67.2 ± 7.1	63.6 ± 5.1	0.092
Disease_duration (years)	11.5 ± 6.7		
PGH (mm)	3.6 ± 1.1	4.4 ± 0.6	0.004
ADC APH/ADC CSF	0.27 ± 0.06	0.26 ± 0.05	0.745
ADC PPH/ADC CSF	0.27 ± 0.04	0.27 ± 0.06	0.883
Prolactin (ng/mL) (normal: 2.7–19.6)	6.6 ± 3.0	6.7 ± 1.8	0.874
LH (IU/L) (normal: 10.9–58.6)	30.5 ± 13.1	31.1 ± 11.1	0.903
DHEA-S (µg/dL) (normal: 8–188)	55.0 ± 40.7	59.6 ± 17.8	0.665
Cortisol (µg/dL) (normal: 6.7–22.6)	8.9 ± 4.6	12.6 ± 4.7	0.040
ACTH (pg/mL) (normal: 0–46)	15.74 ± 7.34	23.81 ± 17.74	0.093
C3 (mg/dL) (normal: 80–180)	138.2 ± 24.3		
C4 (mg/dL) (normal: 16–48)	25.4 ± 8.5		

[1] SD: standard deviation; PGH: pituitary gland height; APH: anterior part of hypothalamus; PPH: posterior part of hypothalamus; ADC: apparent diffusion coefficient; CSF: cerebrospinal fluid; LH: luteinizing hormone; DHEA-S: dehydroepiandrosterone sulfate; ACTH: adrenocorticotropic hormone; C3: Complement 3; C4: Complement 4.

Patients demonstrated different PGH compared with controls (3.6 ± 1.1 mm vs. 4.4 ± 0.6 mm, $p = 0.004$) (Figure 3). Dynamic contrast-enhanced imaging of the HH axis showed a normal enhancement pattern of the posterior pituitary lobe, occurring simultaneously with the straight sinus (9–20 s after contrast administration), and delayed enhancement of the anterior pituitary lobe (40–65 s; mean 49.0 ± 10.2), compared with the expected enhancement at approximately 30 s.

Diffusion tensor imaging (DTI) metrics did not differ between patients and controls. Similarly, no significant differences were observed in most baseline biochemical parameters between the groups. In line with the exploratory scope of these univariate analyses, these remaining variables exhibited values well within standard clinical thresholds and far from the significance margin (Table 1). However, cortisol levels were different in patients compared with controls (8.9 ± 4.6 vs. 12.6 ± 4.7 µg/dL, $p = 0.040$).

In the patient group, linear regression analysis identified only the complement C3 (B = 0.021, SE = 0.009, β = 0.477, t(19) = 2.363, $p = 0.029$) as an independent positive predictor of PGH, explaining 18.6% of its variance ($R^2 = 0.227$, adjusted $R^2 = 0.186$, F(1, 19) = 5.582, $p = 0.029$) (Figure 4).

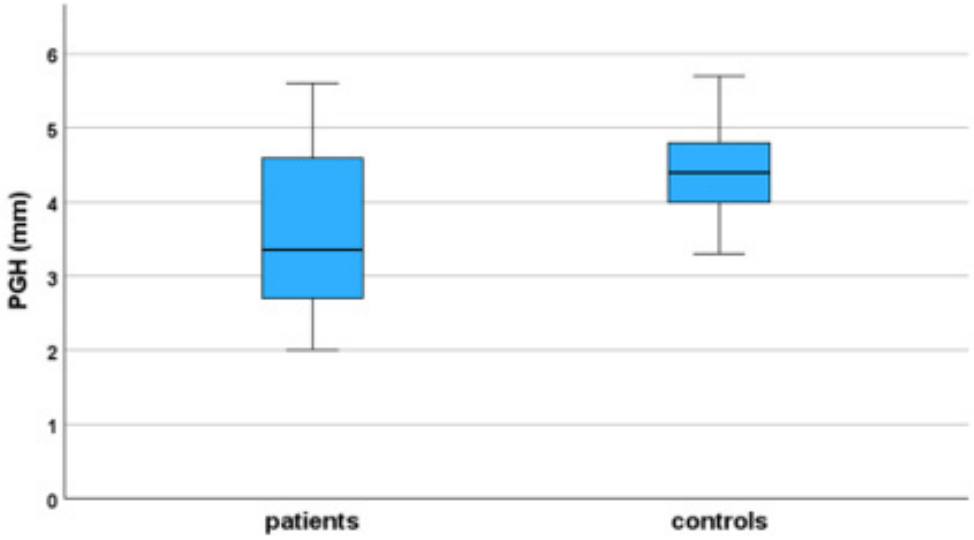


Figure 3. Box plot showing a significantly reduced pituitary gland height (PGH) in postmenopausal women with primary Sjögren's syndrome compared with age- and sex-matched healthy controls.

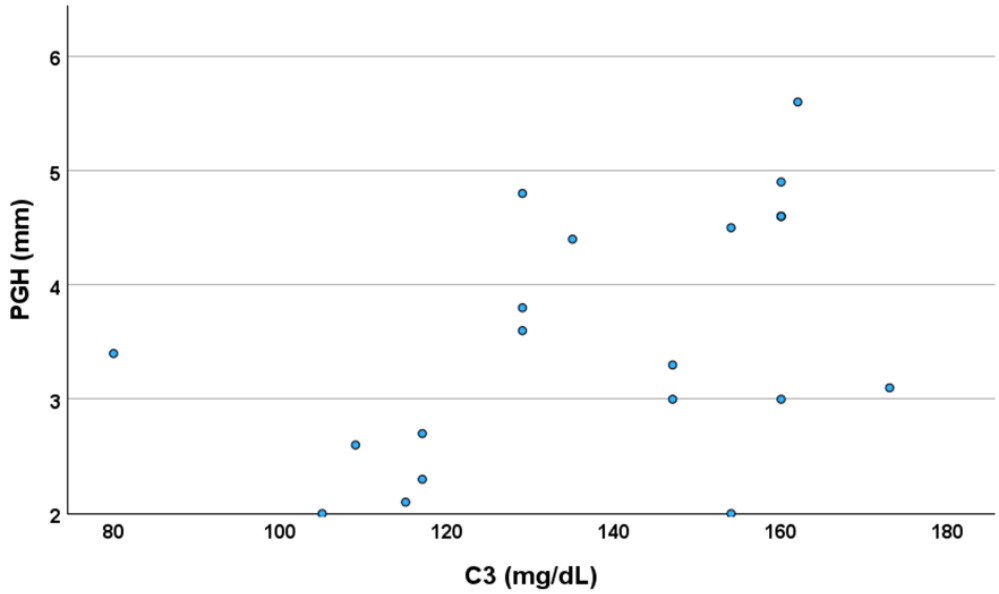


Figure 4. Scatter plot demonstrating the significant positive association between serum complement C3 levels and PGH in postmenopausal women with primary Sjögren's syndrome.

4. Discussion

The main findings of this study in postmenopausal female patients with pSS were decreased PGH, delayed enhancement of the anterior pituitary lobe, a positive association between PGH and C3, and low cortisol levels. Importantly, DTI metrics did not reveal any significant differences between patients and controls, suggesting a lack of microstructural abnormality at the hypothalamic level.

PGH has been proposed as a surrogate marker of pituitary activity, with reduced values associated with adenohypophyseal deficiency [19]. Dynamic contrast enhancement has been used to assess vascularization of the HH axis. The posterior pituitary lobe shows peak enhancement simultaneously with the straight sinus at around 9.2–18.5 s, whereas the anterior pituitary lobe typically enhances within 30 s. This pattern of enhancement reflects the vascular supply of the different parts of the pituitary gland, which arises from two paired arterial systems: the inferior and superior hypophyseal arteries. The inferior hypophyseal

arteries originate from the intracavernous segment of the internal carotid artery, whereas the superior hypophyseal arteries arise just after the internal carotid artery exits the cavernous sinus. The anterior pituitary lobe is supplied by a low-pressure portal system that connects two capillary beds. The primary capillary plexus arises in the median eminence from branches of the superior hypophyseal arteries and drains via the long portal veins of the pituitary stalk into a secondary capillary plexus composed of sinusoids within the anterior pituitary lobe. Hypothalamic hormones released into the primary capillary plexus are transported through the long portal veins into the secondary capillary plexus, where they regulate hormone secretion in the anterior pituitary gland. The posterior lobe has a pure arterial supply from branches of the inferior hypophyseal arteries. After intravenous contrast administration, the posterior pituitary lobe—supplied by a fast-flowing arterial system—enhances first, followed by the pituitary stalk and the median eminence. The anterior pituitary lobe, which is supplied by the low-pressure portal system, enhances last. Any delay in enhancement suggests abnormal pituitary vascularization [15,16]. Previous studies have demonstrated delayed enhancement not only in the posterior pituitary lobe but also in the anterior lobe in patients with diabetes insipidus; these patients subsequently developed GH and TSH deficiencies and exhibited a reduction in pituitary gland height. Furthermore, patients with idiopathic growth hormone deficiency and impaired anterior lobe enhancement have been reported to develop multiple adenohypophyseal hormone deficiencies [22]. In the present study, patients with pSS demonstrated reduced PGH compared with controls, accompanied by delayed enhancement of the anterior pituitary lobe. These findings suggest that vascular impairment may underlie both structural and functional pituitary abnormalities. Histopathological studies in pSS have demonstrated a small-vessel mononuclear inflammatory and ischemic–hemorrhagic vasculopathy [8], which has also been implicated in the development of white matter hyperintensities on brain MRI [6,7]. The anterior pituitary lobe may be particularly vulnerable to such processes due to its complex vascular supply, which includes the hypophyseal arteries and the long and short portal vessels. Inflammatory involvement of this network may lead to hypoxia–ischemia, thereby accounting for both the delayed enhancement pattern and the observed reduction in PGH. In contrast, the absence of detectable hypothalamic microstructural alterations on diffusion tensor imaging (DTI) argues against a primary hypothalamic substrate and instead supports a predominantly vascular–pituitary mechanism. This observation suggests that hypothalamic integrity is relatively preserved and that the observed neuroendocrine dysfunction likely arises at the pituitary level rather than from primary hypothalamic damage.

Our endocrine findings further support this vascular hypothesis. Specifically, lower cortisol levels in the presence of inappropriately “normal” basal ACTH concentrations indicate central HPA axis dysfunction. Under physiological conditions, reduced cortisol levels should trigger a compensatory increase in ACTH secretion via negative feedback. The absence of this response may suggest impaired pituitary sensitivity or a functional disconnection between hypothalamic input and pituitary output, rather than intrinsic hypothalamic structural damage. This interpretation is consistent with previous studies demonstrating a blunted ACTH response to corticotropin-releasing hormone (CRH) stimulation in patients with pSS [12,23,24]. It has been hypothesized that the inflammatory milieu disrupts the pulsatile delivery of hypothalamic signals through the portal system, leading corticotroph cells to enter a state of “functional hibernation.” In this condition, basal hormone secretion is preserved, but the capacity to respond to physiological stress or feedback signals is diminished [12].

Accordingly, the structural alteration (reduced PGH) and the functional impairment (inappropriately normal ACTH despite low cortisol) may represent complementary mani-

festations of a chronic, inflammation-mediated pituitary vasculopathy. A positive correlation was observed between PGH and circulating C3 levels. Complement C3 serves as a marker of systemic complement activation, and its cleavage product C3a has been shown to directly stimulate ACTH release via pituitary receptors [25]. The positive association between C3 and PGH observed in the present study may therefore reflect a state of ongoing complement activation, with C3a as a plausible mediating effector linking immune activity to pituitary morphology. Despite reduced PGH, ACTH levels were relatively preserved, while cortisol levels were lower in patients than in controls. This pattern may reflect a state in which the HPA axis becomes less responsive over time, indicating relative neuroendocrine exhaustion, particularly in the setting of ongoing chronic immune activation. This means that the HPA axis may no longer react as robustly as expected. This could be due to reduced signaling from the hypothalamus (a functional change rather than a structural abnormality), meaning that the initial "trigger" is weaker, and/or changes in how the adrenal glands respond to that signal, resulting in diminished hormonal output.

Taken together, these findings suggest a complex interplay between structural remodeling and functional adaptation. Chronic immune-mediated vascular injury may contribute to reduced PGH, while complement activation—reflected by elevated C3 levels—may exert a partial stimulatory effect on corticotroph function, potentially mediated through its cleavage product C3a. The preservation of ACTH levels despite reduced PGH highlights a dissociation between pituitary structure and function, likely reflecting compensatory mechanisms and residual functional reserve in the context of an intact hypothalamic microstructure.

Overall, these observations are consistent with the concept of pSS as a systemic disease characterized by persistent immune activation and B-cell-driven pathways [26], and they suggest that pituitary morphology and microcirculation may serve as a dynamic marker of the balance between chronic inflammatory damage and ongoing neuroendocrine stimulation, while hypothalamic involvement—if present—appears to be functional rather than structural.

While the cross-sectional design of the present study precludes a definitive declaration of causality, systemic pathophysiological data from the literature strongly suggest that HH axis alterations are secondary manifestations of chronic systemic autoimmunity rather than its upstream driver. The persistent microvascular inflammation and circulating pro-inflammatory cytokines characteristic of pSS likely compromise the anterior pituitary's delicate portal supply, driving corticotroph cells into relative neuroendocrine exhaustion over time. Conversely, no known biological mechanism exists by which primary pituitary structural or vascular delays could upstream trigger the systemic exocrine lymphocytic infiltration and autoantibody profiles that define the disease. Consequently, these structural and perfusional variations are highly probable target-organ manifestations under the strain of chronic systemic autoimmunity [13,26–28].

Moreover, comparison with previous MRI studies of pituitary involvement in systemic autoimmune diseases, such as systemic lupus erythematosus, demonstrates pituitary enlargement, stalk thickening, and altered contrast enhancement. However, MRI abnormalities are often heterogeneous and may be absent despite biochemical evidence of pituitary dysfunction. Our findings support the view that structural imaging changes represent only one aspect of autoimmune pituitary involvement and should be interpreted alongside endocrine and immunological data [29,30].

This study has several limitations, including its relatively small sample size, cross-sectional design, and single-center recruitment from the University of Ioannina, all of which may limit the generalizability of the findings. Although participants were randomly selected, the inclusion of only postmenopausal women minimizes biological variability

related to hormonal fluctuations during the menstrual cycle, which could influence the study outcomes and act as a significant confounding factor.

Although ESSDAI data were not available for this cohort, the study primarily investigated chronic structural pituitary changes rather than current inflammatory disease activity; therefore, the lack of a standardized disease activity assessment is unlikely to have significantly influenced the interpretation of the observed pituitary findings [31].

In addition, our study did not include measurements of C3a levels or C3a receptor expression. Consequently, the proposed complement-mediated mechanism underlying pituitary changes should be regarded as a biologically plausible hypothesis supported by experimental evidence from the literature, rather than a mechanism directly demonstrated in our cohort [25]. Furthermore, the observed association between serum C3 levels and pituitary gland height (PGH) is associative rather than causal. Future studies incorporating measurements of C3a, C3a receptor expression, and PGH are needed to further elucidate the potential role of complement activation in pituitary structural alterations.

The dynamic contrast-enhanced (DCE) MRI analysis in this study relies on a qualitative observation of visual kinetic delays in the anterior pituitary lobe. While a distinct pattern of delayed and flattened enhancement slopes was identified in patients compared to the rapid, sharp peaks observed in healthy controls, formal quantitative or semi-quantitative perfusion metrics—such as time-to-peak (TTP) or wash-in rates—were not calculated. Mathematically modeling anterior pituitary perfusion dynamics poses unique technical challenges, particularly due to the gland's complex dual portal vascular supply and the difficulty of defining an accurate arterial input function (AIF) [32–35]. Because the primary scope of this manuscript focuses on macroscopic structural remodeling (PGH) and hypothalamic microstructural integrity (DTI), a granular, pixel-by-pixel pharmacokinetic curve analysis was deferred. Detailed semi-quantitative and pharmacokinetic modeling of these perfusion dynamics is currently underway as part of a dedicated follow-up neuroimaging investigation to objectively quantify this localized vascular impairment.

5. Conclusions

Postmenopausal patients with pSS exhibit structural, perfusional, and endocrine alterations consistent with HPA axis dysregulation. Reduced PGH and delayed enhancement may suggest inflammation-mediated vascular injury at the pituitary level, supported by the association with C3. Despite low cortisol and inappropriately normal ACTH, DTI showed no hypothalamic microstructural abnormalities, indicating preserved hypothalamic integrity. Overall, these findings point to predominantly pituitary-driven dysfunction, with pituitary imaging markers reflecting underlying microvascular inflammatory damage.

Author Contributions: Conceptualization, M.A., D.N.K. and P.V.; methodology, A.A. and L.A.; software, L.A.; validation, A.Z., E.S., N.K. and N.G.; formal analysis, A.A. and L.A.; investigation, A.Z. and D.N.K.; resources, N.K., G.A. and N.G.; data curation, A.A. and E.S.; writing—original draft preparation, A.Z. and A.A.; writing—review and editing, M.A., D.N.K. and P.V.; supervision, M.A., G.A. and P.V. All authors have read and agreed to the published version of the manuscript.

Funding: This research received no external funding.

Institutional Review Board Statement: The study was reviewed and approved by the Ethics Committee of the University Hospital (No. 328/12-5-2026). The research was conducted in accordance with the guidelines of the Declaration of Helsinki.

Informed Consent Statement: Informed consent was obtained from all subjects involved in the study.

Data Availability Statement: The MRI data supporting the findings of this study were obtained from the University Hospital and are not publicly available due to ethical restrictions. The data

may be made available upon reasonable request, subject to approval by the Ethics Committee of the University Hospital.

Conflicts of Interest: The authors declare no conflict of interest.

Abbreviations

The following abbreviations are used in this manuscript:

HH	Hypothalamic–Hypophyseal
pSS	Primary Sjögren's Syndrome
HPA	Hypothalamic–Pituitary–Adrenal
PGH	Pituitary Gland Height
ACTH	Adrenocorticotropic Hormone
DTI	Diffusion Tensor Imaging
C3	Complement 3
C4	Complement 4
WM	White Matter
MRI	Magnetic Resonance Imaging
LH	Luteinizing Hormone
DHEA-S	Dehydroepiandrosterone Sulfate
TR	Repetition Time
TE	Echo Time
FOV	Field of View
ROI	Region of Interest
ADC	Apparent Diffusion Coefficient
CSF	Cerebrospinal Fluid

References

1. Seror, R.; Bowman, S.J.; Brito-Zeron, P.; Theander, E.; Bootsma, H.; Tzioufas, A.; Gottenberg, J.-E.; Ramos-Casals, M.; Dörner, T.; Ravaud, P.; et al. EULAR Sjögren's syndrome disease activity index (ESSDAI): A user guide. *RMD Open* **2015**, *1*, e000022. [CrossRef] [PubMed]
2. Fox, R.I.; Howell, F.V.; Bone, R.C.; Michelson, P.E. Primary Sjogren syndrome: Clinical and immunopathologic features. *Semin. Arthritis Rheum.* **1984**, *14*, 77–105. [CrossRef] [PubMed]
3. Fauchais, A.-L.; Magy, L.; Vidal, E. Central and peripheral neurological complications of primary Sjögren's syndrome. *La Presse Médicale* **2012**, *41*, e485–e493. [CrossRef] [PubMed]
4. Módis, L.V.; Aradi, Z.; Horváth, I.F.; Bencze, J.; Papp, T.; Emri, M.; Berényi, E.; Bugán, A.; Szántó, A. Central Nervous System Involvement in Primary Sjögren's Syndrome: Narrative Review of MRI Findings. *Diagnostics* **2022**, *13*, 14. [CrossRef] [PubMed]
5. Segal, B.M.; Mueller, B.A.; Zhu, X.; Prosser, R.; Pogatchnik, B.; Holker, E.; Carpenter, A.F.; Lim, K.O. Disruption of brain white matter microstructure in primary Sjögren's syndrome: Evidence from diffusion tensor imaging. *Rheumatology* **2010**, *49*, 1530–1539. [CrossRef] [PubMed]
6. Tzarouchi, L.C.; Zikou, A.K.; Tsifetaki, N.; Astrakas, L.G.; Konitsiotis, S.; Voulgari, P.; Drosos, A.; Argyropoulou, M.I. White matter water diffusion changes in primary Sjögren syndrome. *AJNR Am. J. Neuroradiol.* **2014**, *35*, 680–685. [CrossRef] [PubMed]
7. Tzarouchi, L.C.; Tsifetaki, N.; Konitsiotis, S.; Zikou, A.; Astrakas, L.; Drosos, A.; Argyropoulou, M.I. CNS involvement in primary Sjogren Syndrome: Assessment of gray and white matter changes with MRI and voxel-based morphometry. *AJR Am. J. Roentgenol.* **2011**, *197*, 1207–1212. [CrossRef] [PubMed]
8. Alexander, E.L. Neurologic disease in Sjögren's syndrome: Mononuclear inflammatory vasculopathy affecting central/peripheral nervous system and muscle. A clinical review and update of immunopathogenesis. *Rheum. Dis. Clin. N. Am.* **1993**, *19*, 869–908. [PubMed]
9. Andrianopoulou, A.; Zikou, A.K.; Astrakas, L.G.; Gerolymatou, N.; Xydis, V.; Voulgari, P.; Kiortsis, D.-N.; Argyropoulou, M.I. Functional connectivity and microstructural changes of the brain in primary Sjögren syndrome: The relationship with depression. *Acta Radiol.* **2020**, *61*, 1684–1694. [CrossRef] [PubMed]
10. Xing, W.; Shi, W.; Leng, Y.; Sun, X.; Guan, T.; Liao, W.; Wang, X. Resting-state fMRI in primary Sjögren syndrome. *Acta Radiol.* **2018**, *59*, 1091–1096. [CrossRef] [PubMed]

11. Mavragani, C.P.; Moutsopoulos, H.M. The geoepidemiology of Sjögren's syndrome. *Autoimmun. Rev.* **2010**, *9*, A305–A310. [CrossRef] [PubMed]
12. Johnson, E.O.; Kostandi, M.; Moutsopoulos, H.M. Hypothalamic-pituitary-adrenal axis function in Sjögren's syndrome: Mechanisms of neuroendocrine and immune system homeostasis. *Ann. N. Y. Acad. Sci.* **2006**, *1088*, 41–51. [CrossRef] [PubMed]
13. Mavragani, C.P.; Fragoulis, G.E.; Moutsopoulos, H.M. Endocrine alterations in primary Sjogren's syndrome: An overview. *J. Autoimmun.* **2012**, *39*, 354–358. [CrossRef] [PubMed]
14. Soni, B.K.; Joish, U.K.; Sahni, H.; George, R.A.; Sivasankar, R.; Aggarwal, R. A Comparative Study of Pituitary Volume Variations in MRI in Acute Onset of Psychiatric Conditions. *J. Clin. Diagn. Res.* **2017**, *11*, TC01–TC04. [CrossRef] [PubMed]
15. Shiboski, C.H.; Shiboski, S.C.; Seror, R.; Criswell, L.A.; Labetoulle, M.; Lietman, T.M.; Rasmussen, A.; Scofield, H.; Vitali, C.; Bowman, S.J.; et al. 2016 American College of Rheumatology/European League Against Rheumatism Classification Criteria for Primary Sjögren's Syndrome: A Consensus and Data-Driven Methodology Involving Three International Patient Cohorts. *Arthritis Rheumatol.* **2017**, *69*, 35–45. [CrossRef] [PubMed]
16. Berntsen, E.M.; Haukedal, M.D.; Håberg, A.K. Normative data for pituitary size and volume in the general population between 50 and 66 years. *Pituitary* **2021**, *24*, 737–745. [CrossRef] [PubMed]
17. Tohka, J. Partial volume effect modeling for segmentation and tissue classification of brain magnetic resonance images: A review. *World J. Radiol.* **2014**, *6*, 855–864. [CrossRef] [PubMed]
18. Maghnie, M.; Genovese, E.; Aricò, M.; Villa, A.; Beluffi, G.; Campani, R.; Severi, F. Evolving pituitary hormone deficiency is associated with pituitary vasculopathy: Dynamic MR study in children with hypopituitarism, diabetes insipidus, and Langerhans cell histiocytosis. *Radiology* **1994**, *193*, 493–499. [CrossRef] [PubMed]
19. Argyropoulou, M.I.; Kiortsis, D.N. MRI of the hypothalamic-pituitary axis in children. *Pediatr. Radiol.* **2005**, *35*, 1045–1055. [CrossRef] [PubMed]
20. Baroncini, M.; Jissendi, P.; Catteau-Jonard, S.; Dewailly, D.; Pruvo, J.-P.; Francke, J.-P.; Prevot, V. Sex steroid hormones-related structural plasticity in the human hypothalamus. *Neuroimage* **2010**, *50*, 428–433. [CrossRef] [PubMed]
21. Baroncini, M.; Jissendi, P.; Balland, E.; Besson, P.; Pruvo, J.-P.; Francke, J.-P.; Dewailly, D.; Blond, S.; Prevot, V. MRI atlas of the human hypothalamus. *Neuroimage* **2012**, *59*, 168–180. [CrossRef] [PubMed]
22. Maghnie, M.; Triulzi, F.; Larizza, D.; Preti, P.; Priora, C.; Scotti, G.; Severi, F. Hypothalamic-pituitary dysfunction in growth hormone-deficient patients with pituitary abnormalities. *J. Clin. Endocrinol. Metab.* **1991**, *73*, 79–83. [CrossRef] [PubMed]
23. Johnson, E.O.; Vlachoyiannopoulos, P.G.; Skopouli, F.N.; Tzioufas, A.G.; Moutsopoulos, H.M. Hypofunction of the stress axis in Sjögren's syndrome. *J. Rheumatol.* **1998**, *25*, 1508–1514. [PubMed]
24. Johnson, E.O.; Skopouli, F.N.; Moutsopoulos, H.M. Neuroendocrine manifestations in Sjögren's syndrome. *Rheum. Dis. Clin. N. Am.* **2000**, *26*, 927–949. [CrossRef] [PubMed]
25. Francis, K.; Lewis, B.M.; Akatsu, H.; Monk, P.N.; Cain, S.A.; Scanlon, M.F.; Morgan, B.P.; Ham, J.; Gasque, P. Complement C3a receptors in the pituitary gland: A novel pathway by which an innate immune molecule releases hormones involved in the control of inflammation. *FASEB J.* **2003**, *17*, 2266–2268. [CrossRef] [PubMed]
26. Baldini, C.; Pepe, P.; Quartuccio, L.; Priori, R.; Bartoloni, E.; Alunno, A.; Gattamelata, A.; Maset, M.; Modesti, M.; Tavoni, A.; et al. Primary Sjogren's syndrome as a multi-organ disease: Impact of the serological profile on the clinical presentation of the disease in a large cohort of Italian patients. *Rheumatology* **2014**, *53*, 839–844. [CrossRef] [PubMed]
27. Arzt, E.; Pereda, M.P.; Castro, C.P.; Pagotto, U.; Renner, U.; Stalla, G.K. Pathophysiological role of the cytokine network in the anterior pituitary gland. *Front. Neuroendocr.* **1999**, *20*, 71–95. [CrossRef] [PubMed]
28. Baldini, C.; Fulvio, G.; La Rocca, G.; Ferro, F. Update on the pathophysiology and treatment of primary Sjögren syndrome. *Nat. Rev. Rheumatol.* **2024**, *20*, 473–491. [CrossRef] [PubMed]
29. Xiang, P.; Wu, Q.; Zhang, H.; Luo, C.; Zou, H. Autoimmune Hypophysitis with Systemic Lupus Erythematosus: A Case Report and Literature Review. *Front. Endocrinol.* **2020**, *11*, 579436. [CrossRef] [PubMed]
30. Abdellatif, Z.; Jabareen, R.; Hijazi, N.; Zhalka, A. Lupus-Associated Autoimmune Hypophysitis: A Rare Case. *Cureus* **2025**, *17*, e92222. [CrossRef] [PubMed]
31. Portier, E.; Beydon, M.; Bowman, S.J.; Seror, R. Activity and Damage Indices for Sjögren's Disease. *J. Clin. Med.* **2026**, *15*, 1478. [CrossRef] [PubMed]
32. Gorczyca, W.; Hardy, J. Arterial supply of the human anterior pituitary gland. *Neurosurgery* **1987**, *20*, 369–378. [CrossRef] [PubMed]
33. Espagnet, M.R.; Bangiyev, L.; Haber, M.; Block, K.; Babb, J.; Ruggiero, V.; Boada, F.; Gonen, O.; Fatterpekar, G. High-Resolution DCE-MRI of the Pituitary Gland Using Radial k-Space Acquisition with Compressed Sensing Reconstruction. *AJNR Am. J. Neuroradiol.* **2015**, *36*, 1444–1449. [CrossRef] [PubMed]

34. Kleppestø, M.; Bjørnerud, A.; Groote, I.R.; Kim, M.; Vardal, J.; Larsson, C. Operator dependency of arterial input function in dynamic contrast-enhanced MRI. *Magn. Reson. Mater. Phys. Biol. Med.* **2022**, *35*, 105–112. [CrossRef] [PubMed]
35. Parker, G.J.; Roberts, C.; Macdonald, A.; Buonaccorsi, G.A.; Cheung, S.; Buckley, D.L.; Jackson, A.; Watson, Y.; Davies, K.; Jayson, G.C. Experimentally-derived functional form for a population-averaged high-temporal-resolution arterial input function for dynamic contrast-enhanced MRI. *Magn. Reson. Med.* **2006**, *56*, 993–1000. [CrossRef] [PubMed]

Disclaimer/Publisher's Note: The statements, opinions and data contained in all publications are solely those of the individual author(s) and contributor(s) and not of MDPI and/or the editor(s). MDPI and/or the editor(s) disclaim responsibility for any injury to people or property resulting from any ideas, methods, instructions or products referred to in the content.